Mxi1, a Myc Antagonist, Suppresses Proliferation of DU145 Human Prostate Cells

Mary M. Taj,[1] Rana J. Tawil,[1] Lars D. Engstrom,[1] Zhi Zeng,[2] Clara Hwang,[2] Martin G. Sanda,[2] and Daniel S. Wechsler[1]*

[1]*Division of Pediatric Hematology-Oncology, Department of Pediatrics and Communicable Diseases, University of Michigan School of Medicine, Ann Arbor, Michigan*
[2]*Division of Urology, Department of Surgery, University of Michigan School of Medicine, Ann Arbor, Michigan*

BACKGROUND. Mxi1, an antagonist of c-Myc, maps to human chromosome 10q24-q25, a region altered in a substantial fraction of prostate tumors. Mice deficient for Mxi1 exhibit significant prostate hyperplasia. We studied the ability of Mxi1 to act as a growth suppressor in prostate tumor cells.
METHODS. We infected DU145 prostate carcinoma cells with an Mxi1-expressing adenovirus (AdMxi1) in vitro, and measured Mxi1 expression, cell proliferation, soft agar colony formation, and cell cycle distribution. To explore mechanisms of Mxi1-induced growth arrest, we performed gene expression analysis.
RESULTS. AdMxi1 infection resulted in reduced cell proliferation, reduced soft agar colony formation, and a higher proportion of cells in the G_2/M phase of the cell cycle. This G_2/M growth arrest was associated with elevated levels of cyclin B, and reduced levels of c-*MYC* and *MDM2*.
CONCLUSIONS. The ability of AdMxi1 to suppress prostate tumor cell proliferation supports a role for Mxi1 loss in the pathogenesis of a subset of human prostate cancers. *Prostate 47:194–204, 2001.* © 2001 Wiley-Liss, Inc.

KEY WORDS: **prostate cancer; chromosome 10; c-Myc; adenovirus; G_2/M arrest**

INTRODUCTION

Prostate cancer is the most common cancer in men, and is associated with significant morbidity and mortality. Approximately 200,000 cases of prostate cancer are diagnosed and almost 40,000 men die from prostate cancer in the United States each year [1]. Genetic alterations that contribute to the pathogenesis of prostate tumors include activation of oncogenes and inactivation of tumor suppressor genes. Characteristic gains and losses of chromosomal material, which likely include such genes, are also seen in many cases of prostate cancer [2].

Amplification or overexpression of the c-*MYC* oncogene in many human prostate adenocarcinomas has implicated it in the pathogenesis and progression of prostate cancer [3–7]. Furthermore, c-*MYC*, which encodes a transcription factor of the basic helix-loop-helix/leucine zipper (bHLH/ZIP) family [8,9], is amplified, rearranged, or overexpressed in human prostate cancer cell lines [10-13]. Retrovirally mediated expression of *MYC* in combination with activated *RAS* in the mouse urogenital sinus causes a high frequency

Grant sponsor: American Society for Clinical Oncology; Grant sponsor: Strokes Against Cancer Foundation; Grant sponsor: NICHHD Child Health Research Center; Grant number: 1-P30-HD28820-01; Grant sponsor: NCI; Grant number: 1-P50-CA69568S and 1-P01-CA75136-01A1; Grant sponsor: Howard Hughes Medical Institute; UM–Comprehensive Cancer Center NIH; Grant number: CA46592; Grant sponsor: UM–Multipurpose Arthritic Center NIH; Grant number: AR20557; Grant sponsor; UM–BRCF Core Flow Cytometry Facility.

*Correspondence to: Daniel S. Wechsler, MD, PhD, Section of Pediatric Hematology-Oncology, The University of Michigan, 1500 E. Medical Center Drive, CCGC 4312, Ann Arbor, Michigan 48109. E-mail: dwechsl@umich.edu

Received 31 July 2000; Accepted 18 January 2001

of poorly differentiated prostate cancers in such mice [14]. Chronic overexpression of c-*MYC* in transgenic murine ventral prostate epithelial cells leads to the development of epithelial cell abnormalities similar to those seen in low-grade prostatic intraepithelial neoplasia in humans [15]. Finally, introduction of c-*MYC* antisense transcripts or oligonucleotides into human prostate cell lines both in vitro and in vivo results in reduced cell viability and tumor size [16,17]. Although the overall contribution of c-*MYC* to prostate cancer development and progression remains uncertain [18], these findings clearly implicate increased c-*MYC* expression in prostate cancer pathogenesis.

c-Myc regulates expression of growth-related genes, stimulating cell proliferation and preventing cellular differentiation [19]. Mxi1 is also a transcription factor that belongs to the Mad family of Myc antagonists, which encode proteins that are highly homologous to c-Myc [20–22]. Mxi1 opposes the growth-promoting activity of c-Myc by repressing transcription of c-Myc-activated target genes [23–26]. Mxi1 inhibits the ability of c-Myc to transform cells in vitro [23,27,28], and its expression is associated with cellular differentiation [20,29–31]. By counteracting c-Myc, Mxi1 functions as a growth suppressor, resulting in reduced cell proliferation in vitro [32]. If c-*MYC* overexpression plays a role in the pathogenesis of prostate malignancies, inactivation or loss of *MXI1* might enhance the proliferative effect of c-Myc and contribute to prostate tumor pathogenesis.

Several lines of evidence point to a role for Mxi1 as a potential growth suppressor in the prostate. Transfection of whole chromosome 10 to PC3 prostate cancer cells reduces the tumorigenicity of these cells [33,34], indicating the existence of growth suppressive gene(s) on chromosome 10. We [35] and others [36,37] previously localized the human *MXI1* gene to chromosome 10q24-q25. Deletions resulting in loss of alleles in this region of chromosome 10 are observed in 30–50% of human prostate tumors [18,38–42]. Furthermore, inactivating mutations in the *MXI1* coding sequence have been described in some primary human prostate tumors [43,44]. Finally, *mxi1*-knockout mice, which have a tumorigenic phenotype, demonstrate striking prostate hyperplasia [45]. The enhanced proliferation of prostate epithelium in mice that lack Mxi1 indicates a role for Mxi1 in normal prostate development, and suggests its potential involvement in human prostate neoplasia.

To better define the function of *MXI1* in prostate carcinoma, we have examined the ability of an Mxi1-expressing adenovirus to suppress human prostate cancer cell proliferation. Our demonstration that Mxi1 expression results in markedly decreased proliferation of DU145 prostate cells indicates a role for Mxi1 as a prostate growth suppressor, and supports the hypothesis that loss of Mxi1 activity plays a role in the pathogenesis of a subset of human prostate cancers.

MATERIALS AND METHODS

Cells

DU145 cells, originally derived from a prostate carcinoma brain metastasis, were obtained from the American Type Culture Collection (ATCC, Rockville, MD). DU145 cells are androgen-insensitive, and can form colonies in soft agar [46]. Furthermore, these cells have enhanced expression of c-*MYC*, as well as loss of chromosome 10q [47], and do not have detectable levels of *MXI1* mRNA by Northern blot (Taj and Wechsler, unpublished observations). Cells were maintained in RPMI 1640 (Gibco BRL, Rockville, MD) with 10% heat inactivated fetal bovine serum (HIFBS), 1% penicillin/streptomycin and 1% L-glutamine, and grown in 5% CO_2 at 37°C.

Adenovirus Preparation, Infection, and Optimization

We cloned the human *MXI1* cDNA into pAdRSV4 [48] to generate a human Mxi1-expressing adenovirus (AdMxi1). The pAdRSV4 plasmid includes a constitutive Rous Sarcoma Virus (RSV) promoter to ensure high levels of expression, in an E1-deleted adenovirus backbone. Since reliable, commercial anti-Mxi1 antibodies are not available, we modified the *MXI1* cDNA at its C-terminal end to contain coding sequence for an influenza *h*em*a*gglutinin (HA) peptide epitope (YPYDVPDYA). This HA-tagged protein could then be detected using anti-HA antibodies. After DNA sequencing to confirm appropriate sequence and orientation of the *MXI1*-HA cDNA, replication-incompetent AdMxi1 was prepared by the Virus Core Facility at The University of Michigan, with confirmatory PCR and western blot analysis performed at each step. AdMxi1 was concentrated to a titer of 1×10^{12} particles/ml, and had a replication competent adenovirus (RCA) content of less than 10^{-9}. Control viral preparations included AdLacZ (containing the bacterial β-galactosidase gene), and AdΔE1 (''empty'' virus with a deleted E1 region), both at titers of 1×10^{12} particles/ml. The titer of plaque forming units (pfu) for each virus was estimated to be 1% of the particle number.

Twenty-four hours before viral infection, 10^5 DU145 cells were plated in wells of a 6-well plate. AdMxi1, AdLacZ or AdΔE1 viral particles were suspended in RPMI (with 1% penicillin/streptomycin (p/s) and 1% glutamine (glut) but no HIFBS). Following aspiration

of media from the cells, the viral suspension was added in a total volume of 2 ml. After a 2 hr incubation, the medium was replaced with RPMI containing 5% HIFBS, 1% p/s, and 1% glut. Medium containing 10% HIFBS was replaced 16–18 hr later and every 2–3 day subsequently. To determine the optimal titer for viral infection, DU145 cells were plated in wells of 24-well plates, and infected with a range of AdLacZ titers (MOI (multiplicity of infection) of 10–5000 pfu/cell). Twenty-four hours after infection, cells were washed, fixed with 2% formaldehyde/0.05% glutaraldehyde in PBS, and exposed to the substrate X-gal (5-bromo-4-chloro-3-indolyl-β-D-galactoside; Gibco BRL) at a concentration of 1 mg/ml in PBS with 5 mM potassium ferricyanide, 5 mM potassium ferrocyanide, and 2 mM $MgCl_2$. After X-gal treatment, expression of β-galactosidase results in a blue color, providing a visual measure of the infection efficiency. More than 95% of cells were blue at AdLacZ titers greater than 500 pfu/cell, while uninfected DU145 cells showed no color. Experiments were done at titers of 1250–1750 pfu/cell, since lower titers of either virus (500–1000 pfu/cell) yielded inconsistent differences in growth rate, whereas higher titers (>2500 pfu/cell) resulted in nonspecific toxicity and reduced cell number (Taj and Wechsler, unpublished observations). Because effects of AdLacZ were essentially identical to those seen with AdΔE1, only results for infection with AdΔE1 as a negative control will be presented for clarity.

Western Blot Analysis, Immunofluorescence, and Confocal Microscopy

DU145 cells were plated in 6-well plates at a concentration of 70,000 cells/well. After 24 hr, cells were infected by AdMxi1 at MOI's of 1,000–10,000 pfu/cell. Ninety-six hours following infection, cells were harvested, washed, and subjected to three freeze-thaw cycles. Protein lysates were sonicated, normalized for total protein concentration, mixed with equal volumes of 2 × loading buffer, and boiled for 10 min at 95°C. Samples were electrophoresed on a 12% acrylamide SDS gel, followed by transfer to PVDF membrane (Bio-Rad, Hercules, CA). Mxi1-HA protein was detected with a rabbit polyclonal anti-HA antibody (Santa Cruz Biotechnology, Santa Cruz, CA), followed by goat anti-rabbit IgG HRP (Jackson Immunoresearch Laboratories, West Grove, PA). An HA-tagged Bcl-x_S protein (gift of G. Nunez) was used as a positive control for the HA antibody, and an expected band of approximately 22 kDa was observed (data not shown). The Enhanced Chemiluminescence (ECL; Amersham-Pharmacia, Buckinghamshire, England) system was used for detection according to manufacturer's instructions.

For microscopy studies, DU145 cells were grown on glass cover slips coated with 0.01% poly-L-lysine (Sigma, St. Louis, MO). After 24 hr, cells were infected with AdMxi1 or AdLacZ. Two to four days after infection, cells were cooled on ice for 10 min, washed twice with PBS, and permeabilized with methanol for 7 min at −20°C. After washing twice with PBS at 4°C, cells were incubated for 1 hr with a 1:100 dilution of mouse monoclonal anti-HA antibody (12CA5; Roche, Indianapolis, IN). Following three PBS washes, a 1:50 dilution (in PBS) of secondary antibody (fluorescein-conjugated, goat anti-mouse IgG; Roche) was added to the cells for 1 hr. After three additional PBS washes, Vectashield Mounting Medium (Vector Labs, Burlingame, CA) was applied. Immunofluorescence microscopy was performed using a Nikon Eclipse E600 immunofluorescence microscope. Confocal laser scanning microscopy was performed using a Bio-Rad MRC600 confocal microscope in the Cell Biology Laboratories Core Facility at The University of Michigan.

Soft Agar Clonogenic Assay

The ability of uninfected and virally infected DU145 cells to form colonies in soft agar was determined by minor modification of a previously described procedure [32]. Briefly, a 1:1 mixture of SeaPlaque agarose and SeaKem ME agarose (FMC Bioproducts, Rockland, ME) was used. A 1.4% bottom layer of agarose in RPMI medium (with HIFBS, penicillin/streptomycin, and L-glutamine) in a 100 mm plate was overlaid with 10^5 infected or uninfected DU145 cells resuspended in 0.8% agarose with RPMI (and additives). Tissue culture medium was added atop the agarose layer, and plates were incubated at 37°C in 5% CO_2. Medium was replaced every 3–4 days to prevent drying. Colonies were enumerated 14–21 days later. The soft agar assay was performed three times, with duplicate samples in each assay.

BrdU Incorporation Assay

DU145 cells (5×10^3 cells/well in a 96-well plate) were infected in triplicate with increasing concentrations of AdMxi1 and AdLacZ viruses as described above. After 48 hr, 110 μl of BrdU labeling reagent (1:1,000 dilution; Roche) was added to each well, and cells were incubated for 2 hr at 37° in 5% CO_2. The labeling reagent was then replaced with 200 μl of fixing/denaturing solution, and cells were incubated for 30 min at 25°C. Next, 100 μl of peroxidase-conjugated anti-BrdU antibody (1:100 dilution; Roche) was added, with incubation for 90 min at 25°C. Cells were washed three times, 100 μl of substrate solution were added, and cells were incubated for 30 min at

25°C. Absorbances were first measured at 370 nm (reference wavelength 492 nm) with a SpectraMax ELISA Plate Reader (Molecular Devices, Sunnyvale, CA). After stopping the reactions with 25 μl of 1 M H_2SO_4, absorbances were read at 450 nm (reference wavelength 690 nm).

Flow Cytometry

To evaluate DNA content and expression of Mxi1-HA in infected DU145 cells, 100–400,000 cells were washed in wash buffer (WB: phosphate buffered saline pH 7.2 (PBS)/1% heat-inactivated fetal bovine serum), and fixed with 75% ice-cold ethanol for 2 hr at −20°C. Cells were washed with WB, suspended in 0.25% Triton X-100 in WB for 5 min at 4°C, washed again, and resuspended at a concentration of 10^7 cells/ml. Primary antibody (1:500 rabbit anti-HA (Roche)) was added for 30 min at 25°C, followed by washing with WB. Secondary antibody (donkey anti-rabbit IgG/Cy3 (Jackson Immunoresearch Laboratories)) was added for a 30 min, 25°C incubation, followed by washing with WB. Cell pellets were resuspended in propidium iodide solution (10 μg/ml in PBS) and incubated for a minimum of 10 min. Flow cytometry analysis for DNA content and fluorescence was performed at the University of Michigan Flow Cytometry Core Facility with a Coulter Elite ESP Cell Sorter and accompanying analysis software.

Gene Expression Profiling

The expression levels of cell cycle related genes were evaluated in AdMxi1 infected cells using the GEArray nylon membrane cDNA miniarray System (SuperArray, Bethesda, MD) according to manufacturers instructions. Briefly, mRNA was harvested from AdMxi1- and AdΔE1-infected cells with an Oligotex Direct mRNA Kit (Qiagen, Valencia, CA). After RNA quantitation, cDNA probes were prepared by RT-PCR using GEA primer mix, [α-^{32}P] dCTP and MMLV Reverse Transcriptase. Following prehybridization, labeled cDNA probes were hybridized to Pathway-finder-1 and Cellcycle-1 GEArray membranes at 68°C for 24 hr. After washing, relative transcript abundance was detected with a Molecular Dynamics Storm phosphorimager and quantitated using NIH Image. Hybridizations with each cDNA probe were performed twice.

Statistical Analysis

The two-tailed Student t test was used to assess statistical significance of differences among experimental groups. Probability values of $P < 0.05$ were considered statistically significant.

RESULTS

Exogenous Mxi1 Expression in DU145 Human Prostate Cancer Cells

We assessed the effects of restoring Mxi1 expression to DU145 prostate cancer cells that lack functional Mxi1 expression. To avoid the inefficiency and selection bias associated with plasmid transfection, and to achieve high-level *MXI1* expression in a large percentage of cells, we constructed an E1-deleted (ΔE1), replication-incompetent *MXI1*-expressing adenovirus (AdMxi1). An empty E1-deleted adenovirus (AdΔE1) was used to control for adenoviral infection.

Mxi1-HA protein expression in AdMxi1-infected DU145 cells was assessed by Western blot analysis using an anti-HA antibody. A 36-kDa band corresponding to the size of Mxi1-HA was seen in AdMxi1-infected cell extracts at an MOI of 1,000 pfu/cell (Fig. 1, lane 3). The intensity of this band is not increased when 5,000 pfu/cell are used for infection (lane 4). A band of reduced intensity is seen when as few as 300 pfu/cell were used for infection (Taj and Wechsler, unpublished observations). This HA-specific band is not present in control AdΔE1-infected cells (lane 2), or in uninfected control cells (data not shown). Immunofluorescence microscopy was used to localize the Mxi1-HA protein within infected cells. AdMxi1-infected cells exhibited some cytoplasmic expression and a pronounced speckled pattern of nuclear staining, consistent with the presence of Mxi1 in the nucleus (Fig. 2a). Higher power visualization by confocal laser microscopy confirmed the clumped distribution of nuclear Mxi1-HA in AdMxi1-infected

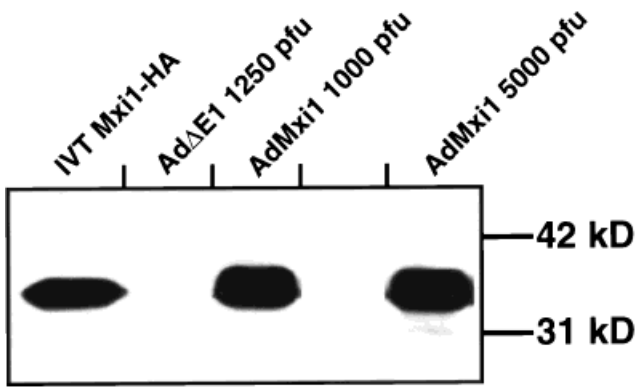

Fig. 1. A 36 kDa Mxi1-HA protein is expressed in AdMxi1-infected DU145 cells. **Lane 1**, in vitro translated (IVT) Mxi1-HA protein; **Lane 2**, cell lysate prepared from DU145 cells infected three days previously with AdΔE1; **Lanes 3 and 4**, cell lysates prepared from DU145 cells infected three days previously with AdMxi1 at the indicated titers. Mxi1-HA protein expression was detected by western blot analysis using a rabbit anti-HA antibody. Mobility of 42 and 31 kDa markers are indicated.

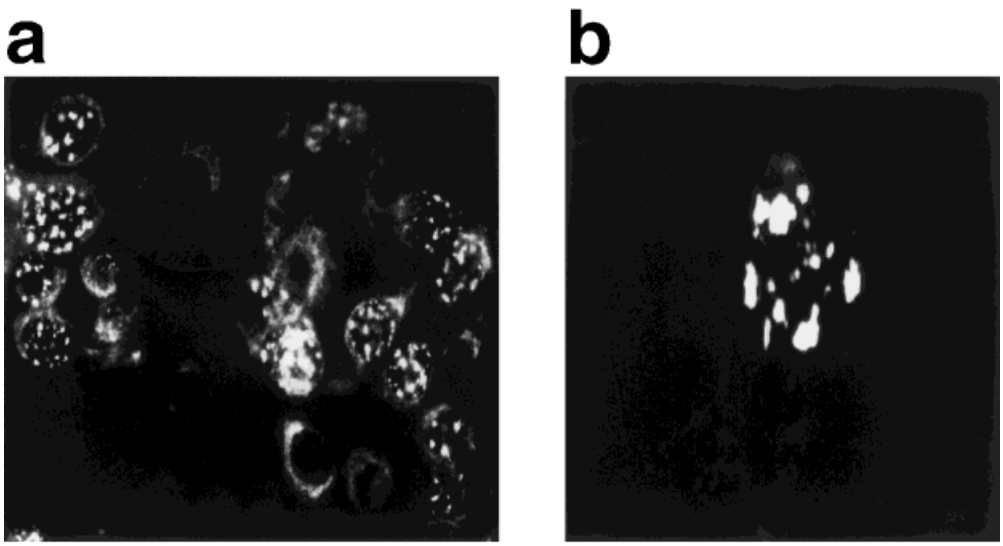

Fig. 2. Mxi1-HA protein distribution in AdMxi1-infected DU145 cells. Three days after infection of DU145 cells with AdMxi1 virus, immunofluorescence (**a**) was performed using a mouse monoclonal anti-HA antibody (magnification × 200). Confocal microscopy (**b**) shows the intranuclear distribution of Mxi1-HA protein at a higher magnification (500x). Note that positive cells have some cytoplasmic fluorescence and striking punctate nuclear fluorescence.

cells (Fig. 2b). No staining was seen in uninfected or AdΔE1-infected cells. These studies indicate that AdMxi1 infection of DU145 cells results in strong expression of Mxi1 protein and transport into the nucleus, where the distribution is consistent with chromatin binding and presumably transcriptional repression activity. The degree of high-level Mxi1-HA expression in infected cells was confirmed by flow cytometry with rabbit anti-HA antibodies, which demonstrated that 75–80% of the AdMxi1-infected cells express Mxi1-HA (see Fig. 5d).

DU145 Proliferation Is Suppressed by Adenoviral Mxi1

Mxi1 expression in DU145 cells by AdMxi1 infection is associated with a marked reduction in growth rate in vitro (Fig. 3). Uninfected DU145 cells (Fig. 3a) and control adenoviral vector AdΔE1-infected cells (Fig. 3b) double their numbers in 24 and 48 hr, respectively, while AdMxi1-infected cells (Fig. 3b) exhibit no appreciable proliferation up to 7 days following infection. On any given day (except day 0), uninfected DU145 cell counts were consistently 1.5–3 times greater than AdΔE1-infected cell numbers, indicating some nonspecific adenovirus-associated toxicity. The growth inhibitory effect of AdMxi1 was apparent and significantly different ($P < 0.003$) from AdΔE1 by the third day postinfection. The growth of AdMxi1-infected cells remained suppressed through day 7 (Fig. 3). After 7 days, a subset of AdMxi1-infected cells began to grow at rates comparable to AdΔE1-infected cells, becoming confluent after 10–13 days. The AdMxi1-infected cells that escaped from growth inhibition showed no residual Mxi1 expression by Western blot (data not shown).

A BrdU incorporation assay was performed to determine whether the increased doubling time of AdMxi1-infected cells was due to reduced cell proliferation. As shown in Figure 4, DU145 cells infected with AdMxi1 show a statistically significant decrease in BrdU incorporation, compared with AdΔE1-infected cells, at all viral titers tested.

To examine the potential of virally infected DU145 cells to form anchorage-independent colonies (a measure of their transformation potential), cells were grown in soft agar. The number of soft agar colonies derived from uninfected DU145 cells was 285 (range 264–308). AdΔE1-infected cells yielded 119 colonies (range 108–136), consistent with nonspecific adenoviral toxicity ($P = 0.0004$). Notably, the number of colonies derived from AdMxi1-infected cells was significantly reduced by nearly 75%, to 31 colonies (range 28–36), in comparison with AdΔE1-infected cells ($P = 0.0007$).

Adenoviral Mxi1 Infection of DU145 Cells Results in G_2/M Arrest

To investigate the mechanism of reduced cell proliferation associated with *MXI1* expression, the cell cycle distributions of control AdΔE1- and AdMxi1-infected DU145 cells were compared. In the control AdΔE1-infected DU145 cells, more than half of the

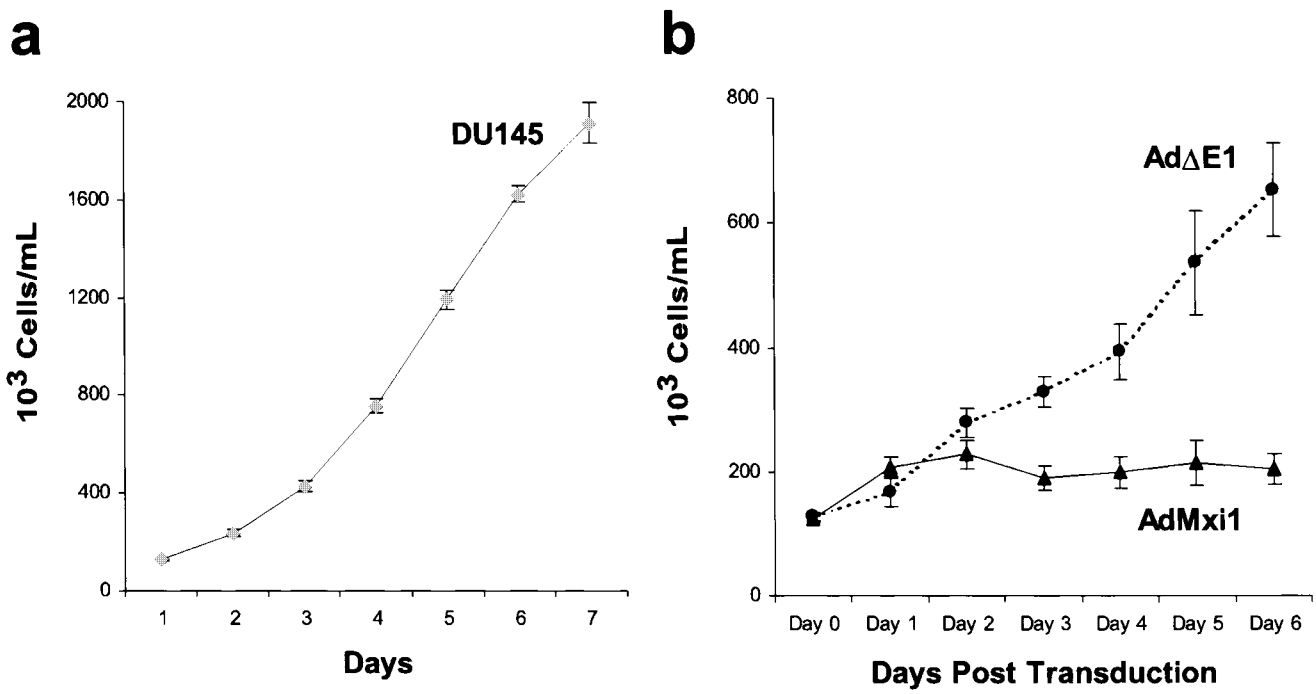

Fig. 3. AdMxiI-infected DUI45 cells exhibit growth suppression in vitro. Growth curves of uninfected DUI45 prostate cells (**a**), or DUI45 cells infected with AdΔEI (—●—) or AdMxiI (—▲—) during log phase of growth (day 0) are shown (**b**). Viable cells were harvested and counted using a Coulter Counter on subsequent days to determine growth curves. AdMxiI-infected cell numbers were significantly lower than AdΔEI-infected cell numbers from day 3–6 (*P*-values of 0.0006, 0.002, 0.003, and 0.00005, respectively). The curves shown represent data from nine separate experiments (±SEM), with infection titers of 1250–1750 pfu/cell.

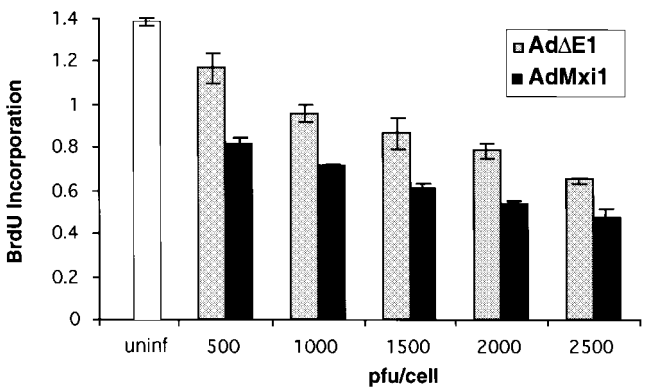

Fig. 4. AdMxiI-infected DUI45 cells incorporate less BrdU than AdΔEI-infected cells. Forty-eight hours after infection with the indicated viral titer of either AdΔEI or AdMxiI, cells were pulsed with BrdU. BrdU incorporation is expressed as OD_{450} units. Uninfected (uninf) DUI45 cells showed a mean BrdU incorporation of 1.4 OD_{450} units (white bar), significantly greater than all infected cells ($P < 0.004$). BrdU incorporation in AdMxiI-infected cells (black bars) was significantly reduced in comparison with AdΔEI-infected cells (shaded bars) at all titers (*P*-values: 0.009 at 500 pfu, 0.003 at 1000 pfu, 0.03 at 1500 pfu, 0.004 at 2000 pfu and 0.01 at 2500 pfu). One representative experiment (of 3 performed) is shown, with triplicate assay results (±SEM).

cells are in G_0/G_1, 30.4% are in S phase, and 15.2% are in G_2/M (Fig. 5a). The profile of uninfected DU145 cells is similar to that shown for AdΔE1-infected cells, with similar percentages of cells in G_0/G_1 (58.1%; $P = 0.10$), S (22.8%; $P = 0.12$), and G_2/M (19.1%; $P = 0.17$). In contrast, in AdMxi1-infected DU145 cells, a significantly lower proportion (30.9%) are in G_0/G_1 ($P = 0.0006$ compared with AdΔE1), with a corresponding relative increase in the number of cells in S phase (37.6%; $P = 0.04$) and G_2/M (31.5%; $P = 0.01$), suggesting that AdMxi1 infection of DU145 cells results in a G_2/M block, as we have previously shown in glioblastoma cells [32]. AdMxi1 does not appear to induce apoptosis, since there is no increase in the number of sub-G_0/G_1 cells. To confirm the lack of AdMxi1-induced apoptosis, we performed a TUNEL assay with uninfected, AdΔE1-infected, and AdMxi1-infected DU145 cells. Using this light microscopy-based qualitative technique, no significant apoptosis was detected in either uninfected or infected DU145 cells: fewer than 5% of cells demonstrated evidence of apoptosis under all three conditions.

Since cyclin B regulates progression through G_2/M, we hypothesized that Mxi1 might alter the level of

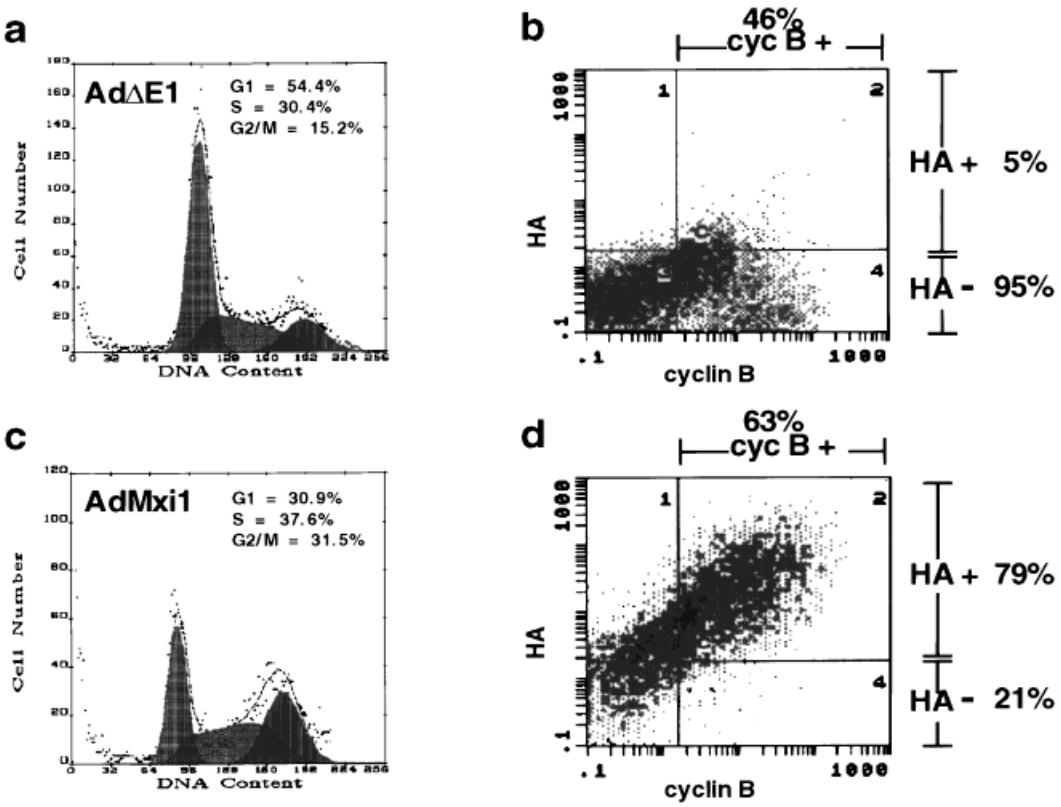

Fig. 5. Flow cytometry analysis of AdΔEI-infected (**a,b**), and AdMxiI-infected (**c,d**) DUI45 cells 72 hr after infection. (a,c) Representative cell cycle profile as measured by PI staining with estimated percentages of cells in G_0/G_1, S, and G_2/M is indicated. Dots indicate cell numbers, dashed curves are extrapolated from dots, and shaded areas are computer-generated estimates of percentage of cells in various phases of the cell cycle. (b,d) Two-color flow cytometric analysis for levels of cyclin B (abscissa) and MxiI-HA (ordinate). AdΔEI-infected cells (b) have only background levels of green fluorescence (5%) corresponding to the MxiI-HA fluorochrome (quadrants I +2), whereas 79% of AdMxiI-infected cells (d) are HA-positive. Cyclin B (quadrants 2 + 4) is detectable in 46% of AdΔEI-infected cells, and 63% of AdMxiI-infected cells. Cyclin B is detectable in 76% of AdMxiI-infected HA-positive cells (double positives, quadrant 2/quadrants 2 + 4), but in only I3% of AdMxiI-infected HA-negative cells (quadrant 4/quadrants 2 + 4). The data shown are from one representative experiment (of six performed); percentages quoted in the text of Results are means (± SEM) from six individual experiments.

cyclin B in comparison with controls, and that altered cyclin B function might be the mechanism for the observed G_2/M block in AdMxi1-infected DU145 cells. Two-color flow cytometric analysis was used to examine the relationship between Mxi1 and cyclin B expression in AdMxi1-infected cells. As indicated in Figure 5, 46% of control AdΔE1-infected cells express cyclin B with only a 5% background of HA + cells. In contrast, 63% of AdMxi1-infected cells express cyclin B, and of these, the majority are also positive for Mxi1-HA expression. In fact, Mxi1-HA expression strongly correlates with expression of cyclin B: $68.5 \pm 6.0\%$ of Mxi1-HA positive cells express cyclin B (double positives, Fig. 5d, quadrant 2), as compared with only $19.7 \pm 5.4\%$ of Mxi1-HA negative cells (Fig. 5d, quadrant 4) ($P = 0.0001$). These results suggest that Mxi1 overexpression perturbs the normal cyclin B expression pattern, and that this perturbation is associated with an altered cell-cycle distribution and a G_2/M blockade.

Finally, as a starting point to explore other possible downstream effectors of Mxi1-induced growth arrest, we surveyed the levels of expression of a panel of cell cycle-related genes in DU145 cells infected by AdMxi1 in comparison with AdΔE1. With RNA from cells infected 48 hr previously, densitometric analysis revealed decreases in the intensity of both c-*MYC* (by 24%) and *MDM2* (by 26%) expression. Although the decreases in c-*MYC* and *MDM2* are relatively modest, they are highly reproducible. In contrast, only minor changes were observed with other genes in the panel (e.g., p53, p21, gadd45) for which no significant alterations were detected. The changes in these patterns of expression were not observed when samples taken 120 hr postinfection were used (data not shown). Taken together, these observations suggest that Mxi1-induced

suppression of proliferation is mediated, at least in part, by well-established regulators of the cell cycle.

DISCUSSION

Several lines of evidence suggest a potential role for Mxi1 as a prostate growth suppressor. First, Mxi1 antagonizes c-Myc [23–28], which is overexpressed in many cases of prostate cancer [3–7]. Second, deletions or rearrangements of the chromosome 10 region to which the *MXI1* gene maps are common in primary prostate tumors [18,38–42]. While *PTEN/MMAC1* [49,50], a chromosome 10q tumor suppressor gene, is thought to play a fundamental role in prostate cancer development, the relative proximity of *MXI1* to *PTEN/MMAC1* suggests that concomitant *MXI1* allelic loss might play a cooperative role in prostate tumor pathogenesis. Third, *MXI1* coding sequence mutations have been described in two separate series of prostate tumors [43,44]. Finally, *mxi1* knockout mice [45] exhibit abnormally hypertrophic prostate glands, with foci of enlarged and complex glandular structures, hypercellular acini, dysplastic cells, and occasional mitotic figures, supporting the notion that Mxi1 plays a role in prostate development. Although they display no overt prostate neoplastic changes, these mice do spontaneously develop malignant lymphomas, indicating that Mxi1 may play a role as a tumor suppressor gene in vivo [51]. The ability of Mxi1 to ''balance'' and antagonize the activity of c-Myc, and the resultant increased, relatively unopposed c-Myc activity in *mxi1* knockout mice may contribute to these changes. The goal of the present study was to test the effectiveness of an Mxi1-expressing adenovirus in reducing proliferation of prostate tumor cells in vitro.

We previously demonstrated the ability of Mxi1 to suppress growth of glioblastoma cells using an inducible plasmid expression vector [32]. In the present studies in human prostate cells, we used an adenovirus vector containing the *MXI1* cDNA to infect DU145 cells. Because of the lack of an effective anti-Mxi1 antibody, we tagged Mxi1 with an influenza *h*em*a*gglutinin (HA) peptide epitope to enable detection; since results similar to those using a native Mxi1 protein were obtained [32], the presence of a C-terminal HA moiety apparently does not interfere with Mxi1 function. Using AdMxi1, we achieved an infection efficiency of 90–95%, with 75–80% of cells expressing Mxi1 protein in the nucleus 48 hr after infection. Enhanced Mxi1 expression led to a significant reduction in growth rate during the first week post-infection. After 7 days, AdMxi1-infected cells tended to grow at rates comparable to AdΔE1-infected cells, and after 10–13 days, confluent AdMxi1-infected cells showed no residual Mxi1 expression by western blot. The mechanism of outgrowth of Mxi1-HA negative cells is not known. While the outgrowth might be due to the recovery and emerging predominance of a minimal subset of uninfected cells, it could also be related to loss of the ability of infected cells to express the Mxi1-HA protein, perhaps by promoter methylation.

AdMxi1 infection of DU145 prostate carcinoma cells led to a nearly 75% reduction in the number of colonies in soft agar when compared to colonies from cells infected with the control AdΔE1 adenovirus. Since anchorage-independent growth in soft agar correlates with tumorigenicity in vivo, this finding indicates that Mxi1 suppresses factors necessary for tumor production. There was also a reduction in BrdU incorporation in AdMxi1-infected cells that correlated with the reduced proliferation induced by AdMxi1. The observed reduction in proliferation was not due to apoptosis, since we did not detect an increase in the sub-G_0/G_1 peak by flow cytometry or in apoptotic nuclei using the TUNEL assay. However, using flow cytometry, we did detect an increased proportion of cells in the S and G_2/M phases of the cell cycle. This observation of a G_2/M arrest as one possible mechanism by which *MXI1* suppresses proliferation is intriguing, since we saw a similar Mxi1-dependent effect in a completely different cell line (U87MG glioblastoma) using a different method of expression (transfection with an inducible *MXI1* plasmid) of a non-HA-tagged Mxi1 protein [32]. Notably, this effect on the cell cycle is different from that produced with the highly homologous Mad1 protein [52], suggesting that these Myc antagonists may have different gene targets.

In investigating the mechanism of the G_2/M arrest, we found increased levels of cyclin B after adenoviral Mxi1 expression. Dephosphorylation of cyclin B is required for transition through the G_2/M phase of the cell cycle. Perturbation of normal cyclin B levels in the setting of Mxi1 overexpression may prevent exit from this stage of the cell cycle. Indeed, elevated levels of cyclin B have been described in G_2/M arrest [53,54]. It is not known whether Mxi1 expression directly results in increased cyclin B expression, or whether cyclin B is elevated indirectly as a result of the G_2/M block. The specific mechanisms for increased cyclin B expression (e.g., whether it is transcriptionally or posttranscriptionally mediated) remain to be elucidated. In addition, we observed reduced levels of c-*MYC* and *MDM2* after adenoviral Mxi1 expression. The observed reduction in c-*MYC* mRNA expression is consistent with the previously described direct transcriptional repression of the c-Myc promoter by Mxi1 [55]. Since c-Myc overexpression promotes proliferation and transition through G_2/M, reduced c-Myc as seen in

AdMxi1-infected cells may inhibit this progression. Indeed, many of the effects of Mxi1 may result from direct or indirect misregulation of c-Myc. Finally, since Mdm2 negatively regulates p53-mediated growth suppression, Mxi1-induced downregulation of *MDM2* might enhance p53-mediated growth suppression [56,57]. Whether this is a direct (i.e., transcriptional) effect of Mxi1 overexpression, or merely a reflection of an ongoing G_2/M block is unclear at the present time. The absence of changes in these patterns of expression by 120 hr after infection with AdMxi1 may be attributable to transcriptional repression by Mxi1 that occurs during a relatively short window of time. Alternatively, a population of cells with reduced Mxi1 expression may already begin to appear at this time.

Alterations in levels of other cell cycle proteins in the presence of Mxi1 overexpression remain to be evaluated. For example, since c-Myc activates transcription and expression of the cdc25A CDK-activating phosphatase [58], downregulation of this protein by Mxi1 might also contribute to the observed cell cycle arrest. Nevertheless, Mxi1-induced alterations in cyclin B, c-Myc, and Mdm2 indicate their potential involvement in G_2/M growth arrest.

CONCLUSIONS

Prostate cancer, which is most common in later life, arises as a result of a multistep process of oncogene-activating and tumor suppressor gene-inactivating events. It is likely that a number of cooperating genetic lesions contribute to tumor development, with possible involvement of Mxi1 in a subset of tumors. Whether Mxi1 is involved early or late in the process is presently unknown. We have demonstrated prostate cancer cell growth inhibition by AdMxi1, with resultant G_2/M arrest, associated with increased expression of cyclin B and reduced expression of c-Myc and Mdm2. These findings indicate a growth suppressor role for Mxi1 in prostate cancer. The ability of adenovirus-mediated Mxi1 expression to reduce DU145 prostate cell proliferation provides a rationale for future studies to develop in vivo methods of Mxi1 delivery as a strategy for reducing malignant prostate cancer growth and progression.

ACKNOWLEDGMENTS

We thank K. Cherian (University of Michigan Adenovirus Core) for help in viral production, and M. KuKuruga (University of Michigan Flow Cytometry Core) for assistance in flow cytometry analysis. We appreciate the constructive input of L. Benson, T. Carey, C. Dang, G, Nunez, K. Pienta, S. Wechsler, and R. Wechsler-Reya.

This study was supported in part by An American Society for Clinical Oncology Young Investigator Award, the Strokes Against Cancer Foundation, NICHHD Child Health Research Center Grant 1-P30-HD28820-01, and NCI Prostate SPORE 1-P50-CA69568S (to D.S.W.); a Howard Hughes Medical Institute Research Training Fellowship for Medical Students (to C.H.); an American Society for Clinical Oncology Career Development Award, and NCI 1-PO1-CA75136-01A1 (to M.G.S.); and by the UM–Comprehensive Cancer Center NIH CA46592, the UM–Multipurpose Arthritic Center NIH AR20557 and the UM–BRCF Core Flow Cytometry facility.

REFERENCES

1. Landis SH, Murray T, Bolden S, Wingo PA. Cancer statistics, 1998. CA Cancer J Clin 1998;48:6–29.
2. Dong J-T, Isaacs WB, Isaacs JT. Molecular advances in prostate cancer. Curr Opinion in Oncology 1997;9:101–107.
3. Fleming WH, Hamel A, MacDonald R, Ramsey E, Pettigrew NM, Johnston B, Dodd JG, Matusik RJ. Expression of the c-myc protooncogene in human prostatic carcinoma and benign prostatic hyperplasia. Cancer Res 1986;46:1535–1538.
4. Buttyan R, Sawczuk IS, Benson MC, Siegal JD, Olsson CA. Enhanced expression of the c-myc protooncogene in high-grade human prostate cancers. Prostate 1987;11:327–337.
5. Fox SB, Persad RA, Royds J, Kore RN, Silcocks PB, Collins CC. p53 and c-myc expression in stage A1 prostatic adenocarcinoma: useful prognostic determinants? J Urol 1993;150:490–494.
6. Qian J, Jenkins RB, Bostwick DG. Detection of chromosomal anomalies and c-myc gene amplification in the cribriform pattern of prostatic intraepithelial neoplasia and carcinoma by fluorescence in situ hybridization. Mod Pathol 1997;10:1113–1119.
7. Jenkins RB, Qian J, Lieber MM, Bostwick DG. Detection of c-myc oncogene amplification and chromosomal anomalies in metastatic prostatic carcinoma by fluorescence in situ hybridization. Cancer Res 1997;57:524–531.
8. Potter M, Marcu KB. The c-myc story: where we've been, where we seem to be going. Curr Top Microbiol Immunol 1997;224:1–17.
9. Facchini LM, Penn LZ. The molecular role of Myc in growth and transformation: recent discoveries lead to new insights. FASEB J 1998;12:633–651.
10. Nag A, Smith RG. Amplification, rearrangement, and elevated expression of c-myc in the human prostatic carcinoma cell line LNCaP. Prostate 1989;15:115–122.
11. Wolf DA, Kohlhuber F, Schulz P, Fittler F, Eick D. Transcriptional down-regulation of c-myc in human prostate carcinoma cells by the synthetic androgen mibolerone. Br J Cancer 1992;65:376–382.
12. Yamazaki H, Schneider E, Myers CE, Sinha BK. Oncogene overexpression and de novo drug-resistance in human prostate cancer cells. Biochim Biophys Acta 1994;1226:89–96.
13. Asadi FK, Sharifi R. Effects of sex steroids on cell growth and c-myc oncogene expression in LN-CaP and DU-145 prostatic carcinoma cell lines. Int Urol Nephrol 1995;27:67–80.
14. Thompson TC, Truong LD, Timme TL, Kadmon D, McCune BK, Flanders KC, Scardino PT, Park SH. Transgenic models for the study of prostate cancer. Cancer 1993;71:1165–1171.

15. Zhang X, Lee C, Ng PY, Rubin M, Shabsigh A, Buttyan R. Prostatic neoplasia in transgenic mice with prostate-directed overexpression of the c-myc oncoprotein. Prostate 2000;43:278–285.
16. Balaji KC, Koul H, Mitra S, Maramag C, Reddy P, Menon M, Malhotra RK, Laxmanan S. Antiproliferative effects of c-myc antisense oligonucleotide in prostate cancer cells: a novel therapy in prostate cancer. Urology 1997;50:1007–1015.
17. Steiner MS, Anthony CT, Lu Y, Holt JT. Antisense c-myc retroviral vector suppresses established human prostate cancer. Hum Gene Ther 1998;9:747–755.
18. Isaacs WB, Bova GS. Prostate cancer. In: B. Vogelstein B, Kinzler KW, editors. The genetic basis of human cancer. New York: McGraw-Hill; 1998;653–660.
19. Dang CV. c-Myc target genes involved in cell growth, apoptosis, and metabolism. Mol Cell Biol 1999;19(1):1–11.
20. Zervos AS, Gyuris J, Brent R. Mxi1, a protein that specifically interacts with Max to bind Myc-Max recognition sites. Cell 1993;72:223–232.
21. Ayer DE, Kretzner L, Eisenman RN. Mad: a heterodimeric partner for Max that antagonizes Myc transcriptional activity. Cell 1993;72:211–222.
22. Hurlin PJ, Queva C, Koskinen PJ, Steingrimsson E, Ayer DE, Copeland NG, Jenkins NA, Eisenman RN. Mad3 and Mad4: novel Max-interacting transcriptional repressors that suppress c-myc dependent transformation and are expressed during neural and epidermal differentiation. EMBO J 1995;14: 5646–5659.
23. Schreiber-Agus N, Chin L, Chen K, Torres R, Rao G, Guida P, Skoultchi AI, DePinho RA. An amino-terminal domain of Mxi1 mediates anti-Myc oncogenic activity and interacts with a homolog of the yeast transcriptional repressor SIN3. Cell 1995;80:777–786.
24. Rao G, Alland L, Guida P, Schreiber-Agus N, Chen K, Chin L, Rochelle JM, Seldin MF, Skoultchi AI, DePinho RA. Mouse Sin3A interacts with and can functionally substitute for the amino-terminal repression of the Myc antagonist Mxi1. Oncogene 1996;12:1165–1172.
25. Alland L, Muhle R, Hou H Jr, Potes J, Chin L, Schreiber-Agus N, DePinho RA. Role for N-CoR and histone deacetylase in Sin3-mediated transcriptional repression. Nature 1997;387:49–55.
26. O'Hagan RC, Schreiber-Agus N, Chen K, David G, Engelman JA, Schwab R, Alland L, Thomson C, Ronning DR, Sacchettini JC, Meltzer P, DePinho RA. Gene-target recognition among members of the myc superfamily and implications for oncogenesis. Nat Genet 2000;24:113–119.
27. Lahoz EG, Xu L, Schreiber-Agus N, DePinho RA. Suppression of Myc, but not E1a, transformation activity by Max-associated proteins, Mad and Mxi1. Proc Natl Acad Sci USA 1994;91:5503–5507.
28. Schreiber-Agus N, Chin L, Chen K, Torres R, Thomson CT, Sacchettini JC, DePinho RA. Evolutionary relationships and functional conservation among vertebrate Max-associated proteins: the zebra fish homolog of Mxi1. Oncogene 1994;9: 3167–3177.
29. Larsson LG, Bahram F, Burkhardt H, Luscher B. Analysis of the DNA-binding activities of Myc/Max/Mad network complexes during induced differentiation of U-937 monoblasts and F9 teratocarcinoma cells. Oncogene 1997;15:737–748.
30. Delgado MD, Lerga A, Canelles M, Gomez-Casares MT, Leon J. Differential regulation of Max and role of c-Myc during erythroid and myelomonocytic differentiation of K562 cells. Oncogene 1995;10:1659–1665.
31. Queva C, Hurlin PJ, Foley KP, Eisenman RN. Sequential expression of the MAD family of transcriptional repressors during differentiation and development. Oncogene 1998;16(8): 967–977.
32. Wechsler DS, Shelly CA, Petroff CA, Dang CV. MXI1, a putative tumor suppressor gene, suppresses growth of human glioblastoma cells. Cancer Res 1997;57:4905–4912.
33. Ichikawa T, Nihei N, Kuramochi H, Kawana Y, Killary AM, Rinker Schaeffer CW, Barrett JC, Isaacs JT, Kugoh H, Oshimura M, Shimazaki J. Metastasis suppressor genes for prostate cancer. Prostate Suppl 1996;6:31–35.
34. Murakami YS, Albertsen H, Brothman AR, Leach RJ, White RL. Suppression of the malignant phenotype of human prostate cancer cell line PPC-1 by introduction of normal fragments of human chromosome 10. Cancer Res 1996;56:2157–2160.
35. Wechsler DS, Hawkins AL, Li X, Jabs EW, Griffin CA, Dang CV. Localization of the human Mxi1 transcription factor gene (MXI1) to chromosome 10q24-q25. Genomics 1994;21:669–672.
36. Edelhoff S, Ayer DE, Zervos AS, Steingrimsson E, Jenkins NA, Copeland NG, Eisenman RN, Brent R, Disteche CM. Mapping of two genes encoding members of a distinct subfamily of MAX interacting proteins: MAD to human chromosome 2 and mouse chromosome 6, and MXI1 to human chromosome 10 and mouse chromosome 19. Oncogene 1994;9:665–668.
37. Shapiro DN, Valentine V, Eagle L, Yin X, Morris SW, Prochownik EV. Assignment of the human MAD and MXI1 genes to chromosomes 2p12-p13 and 10q24-q25. Genomics 1994;23:282–285.
38. Brothman AR, Peehl DM, Patel AM, McNeal JE. Frequency and pattern of karyotypic abnormalities in human prostate cancer. Cancer Res 1990;50:3795–3803.
39. Carter BS, Ewing CM, Ward WS, Treiger BF, Aalders TW, Schalken JA, Epstein JI, Isaacs WB. Allelic loss of chromosomes 16q and 10q in human prostate cancer. Proc Natl Acad Sci USA 1990;87:8751–8755.
40. Lundgren R, Mandahl N, Heim S, Limon J, Henrikson H, Mitelman F. Cytogenetic analysis of 57 primary prostatic adenocarcinomas. Genes Chromosomes Cancer 1992;4:16–24.
41. Ittmann M. Allelic loss on chromosome 10 in prostate adenocarcinoma. Cancer Res 1996;56:2143–2147.
42. Lacombe L, Orlow I, Reuter VE, Fair WR, Dalbagni G, Zhang ZF, Cordon-Cardo C. Microsatellite instability and deletion analysis of chromosome 10 in human prostate cancer. Int J Cancer 1996;69:110–113.
43. Eagle LR, Yin X, Brothman AR, Williams BJ, Atkin NB, Prochownik EV. Mutation of the MXI1 gene in prostate cancer. Nat Genet 1995;9:249–255.
44. Prochownik EV, Eagle Grove L, Deubler D, Zhu XL, Stephenson RA, Rohr LR, Yin X, Brothman AR. Commonly occurring loss and mutation of the MXI1 gene in prostate cancer. Genes Chromosomes Cancer 1998;22:295–304.
45. Schreiber-Agus N, Meng Y, Hoang T, Hou H Jr, Chen K, Greenberg R, Cordon-Cardo C, Lee HW, DePinho RA. Role of Mxi1 in ageing organ systems and the regulation of normal and neoplastic growth. Nature 1998;393:483–487.
46. Stone KR, Mickey DD, Wunderli H, Mickey GH, Paulson DF. Isolation of a human prostate carcinoma cell line (DU 145). Int J Cancer 1978;21:274–281.
47. Bernardino J, Bourgeois CA, Muleris M, Dutrillaux AM, Malfoy B, Dutrillaux B. Characterization of chromosome changes in two human prostatic carcinoma cell lines (PC-3 and DU145) using chromosome painting and comparative genomic hybridization. Cancer Genet Cytogenet 1997;96:123–128.

48. Crystal RG. Transfer of genes to humans: early lessons and obstacles to success. Science 1995;270:404–410.
49. Li J, Yen C, Liaw D, Podsypanina K, Bose S, Wang SI, Puc J, Miliaresis C, Rodgers L, McCombie R, Bigner SH, Giovanella BC, Ittmann M, Tycko B, Hibshoosh H, Wigler MH, Parsons R. PTEN, a putative protein tyrosine phosphatase gene mutated in human brain, breast, and prostate cancer. Science 1997;275:1943–1947.
50. Steck PA, Pershouse MA, Jasser SA, Yung WK, Lin H, Ligon AH, Langford LA, Baumgard ML, Hattier T, Davis T, Frye C, Hu R, Swedlund B, Teng DH, Tavtigian SV. Identification of a candidate tumour suppressor gene, MMAC1, at chromosome 10q23.3 that is mutated in multiple advanced cancers. Nat Genet 1997;15:356–362.
51. Foley KP, Eisenman RN. Two MAD tails: what the recent knockouts of Mad1 and Mxi1 tell us about the MYC/MAX/MAD network. Biochim Biophys Acta 1999;1423:M37–47.
52. Chen J, Willingham T, Margraf LR, Schreiber-Agus N, DePinho RA, Nisen PD. Effects of the MYC oncogene antagonist, MAD, on proliferation, cell cycling and the malignant phenotype of human brain tumour cells. Nat Med 1995;1:638–643.
53. Maity A, Hwang A, Janss A, Phillips P, McKenna WG, Muschel RJ. Delayed cyclin B1 expression during the G2 arrest following DNA damage. Oncogene 1996;13:1647–1657.
54. Suzuki M, Hosaka Y, Matsushima H, Goto T, Kitamura T, Kawabe K. Butyrolactone I induces cyclin B1 and causes G2/M arrest and skipping of mitosis in human prostate cell lines. Cancer Lett 1999;138:121–130.
55. Lee TC, Ziff EB. Mxi1 is a repressor of the c-Myc promoter and reverses activation by USF. J Biol Chem 1999;274:595–606.
56. Momand J, Zambetti GP, Olson DC, George D, Levine AJ. The mdm-2 oncogene product forms a complex with the p53 protein and inhibits p53-mediated transactivation. Cell 1992;69:1237–1245.
57. Reifenberger G, Liu L, Ichimura K, Schmidt EE, Collins VP. Amplification and overexpression of the MDM2 gene in a subset of human malignant gliomas without p53 mutations. Cancer Res 1993;53:2736–2739.
58. Galaktionov K, Chen X, Beach D. Cdc25 cell-cycle phosphatase as a target of c-myc. Nature 1996;382:511–517.